A bimetallic pillared-layer metal–organic coordination framework with a 3D biporous structure†

Tapas Kumar Maji,* Suchetan Pal, K. L Gurunatha, A. Govindaraj and C. N. R. Rao*

Received 20th October 2008, Accepted 3rd April 2009
First published as an Advance Article on the web 20th April 2009
DOI: 10.1039/b818498d

A novel bimetallic [Mn(II)–Fe(III)] 3D biporous pillared-layer metal–organic coordination framework constructed by a cyanometallate anion ($[Fe(CN)_6]^{3-}$) and an organic linker (4,4′-bipy) is found to exhibit permanent porosity with excellent size selective vapour sorption properties and H_2-storage capability.

The design and synthesis of metal–organic coordination frameworks has attracted much attention as promising functional materials.[1] Porous frameworks with novel spin carriers may exhibit dual functionality in a single system and guest-induced magnetic modulation have recently been demonstrated.[2] The well-studied inorganic metalloligand, hexacyanometallate ($[M(CN)_6]^{n-}$), forms versatile networks with different metal ions, giving rise to a family of magnetic materials[2b,c,d,3] and Prussian blue analogues also exhibit porous functionality.[4] Metal–organic frameworks, with tunable pore sizes, have been found to exhibit size selective adsorption and separation of small molecules[1] and as a promising H_2-storage materials.[5] Selective separation and isolation of small molecules on the basis of polarity or size, such as separation between alcohols are of great industrial, and environmental importance.[6] On the other hand, for storage of a large amount of H_2, one of the strategies is to embed coordinatively unsaturated metal sites on the pore surfaces, which can interact more strongly than that the weak dispersion forces or the H-bond. Evidence of stronger binding of H_2 to the Cu(II)/Ni(II)/Mn(II) open metal sites have been reported.[7] In this communication, we report the rational design, synthesis, structure and magnetic properties of a bimetallic pillared-layer framework compound, $\{[Mn_3(4,4'\text{-bipy})_3(H_2O)_4][Fe(CN)_6]_2.2(4,4'\text{-bipy}).3(H_2O)\}_n$ (**1**) with a 3D porous structure exhibiting selective sorption properties as well as hydrogen storage characteristics. The systematic design of 3D microporous framework of M(II) exploiting the bridging potential of $[M(CN)_6]^{n-}$ in combination with organic pillar modules is yet to be reported.

Brown-coloured square block type single crystals of **1** were grown by the slow diffusion of $K_3[Fe(CN)_6]$ and 4,4′-bipy with $MnCl_2$ in $EtOH/H_2O$ medium (see ESI).† The IR spectrum of **1** shows two $\nu(C{\equiv}N)$ bands at 2067 cm^{-1} and 2129 cm^{-1} corresponding to the bridging and terminal cyanide groups, respectively (Fig. S1).†

X-ray crystallographic structure determination‡ reveals that **1** is a neutral 3D coordination architecture of Mn(II) built by ($[Fe(CN)_6]^{3-}$) and 4,4′-bipy with the formulation $\{[Mn_3(4,4'\text{-bipy})_3(H_2O)_4][Fe(CN)_6]_2.2(4,4'\text{-bipy})\cdot 3(H_2O)\}_n$ (**1**). There are two crystallographically independent Mn (Mn1 and Mn2) atoms in the asymmetric unit and each octahedral Mn1 is coordinated to three CN groups from three different $Fe(CN)_6^{3-}$, one water molecule (O1) and two 4,4′-bipy, whereas each octahedral Mn2 is coordinated two CN groups, two 4,4′-bipy and two water molecules (O2, O2*) (Fig. S2 and 1a).† Both Mn1 and Mn2 are slightly distorted from the perfect octahedron as reflected in the *cisoid* angles (83.45(17)–92.34(19)° for Mn1 and 85.08(13)–94.92(13)° for Mn2). The Mn-N and Mn-O bond distances are in the range of 2.158(5)–2.269(3) Å and 2.200(4)–2.263(3) Å, respectively. In the 2D layers, the twelve membered $Mn1_2Fe1_2(CN)_4$ ring surrounded by six eighteen-membered $Mn1Mn2_2Fe1_3(CN)_{12}$ rings and each 2D layer connected by the 4,4′-bipy linker through the Mn(II) centres forms a 3D pillared-layer network with two kind of channels along the *c*-axis (Fig. 1 and Fig. S3).† Examination with TOPOS[8] reveals that **1** is a tri-nodal (4-c)3(5-c)2-periodic 3D net formed by 5-connected (5-c) Mn- nodes, 4-c Fe-nodes and 2-c 4,4′-bipy and CN linkers. In a layer, the vertex symbol for Mn1, Mn2 and Fe1 points are represented by Schläfli symbols, $\{4.6^8.8\}$, $\{6^5.8\}$ and $\{4.6^5\}$, respectively. Further examination shows that **1** adopts a unprecedented network topology with the Schläfli symbol $\{4.6^5\}2\{4.6^8.8\}2\{6^5.8\}$. The square-shaped smaller channel (2.8×2.2 Å^2) contains two water molecules and the large channel (7.7×5.5 Å^2) contains one water and 4,4′-bipy molecule as guests, both of which providing about 35.1% void spaces to the total crystal volume.[9] Thus, **1** acts as a biporous host (Fig. 1a). Upon removal of the coordinated water molecules, framework shows 40.3% void space to the total volume with coordinatively unsaturated Mn(II)

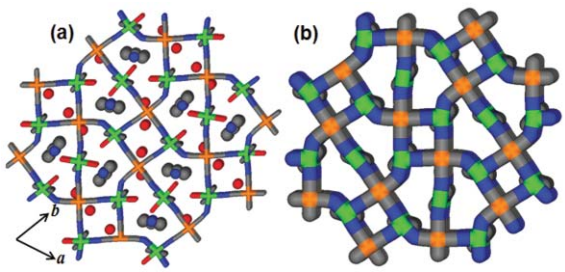

Fig. 1 (a) 3D network of **1** showing two kinds of channels along the crystallographic *c*-axis. The square small channel accommodates water molecules and the larger channel is occupied by the free 4,4′-bipy and water molecules; (b) Views of the pore: stick diagram of **1** showing two different pores along the *c*-axis. The guest molecules (water and 4,4′-bipy) and coordinated water molecules have been omitted.

Chemistry and Physics of Materials Unit, Jawaharlal Nehru Centre for Advanced Scientific Research, Jakkur, Bangalore, 560 064, India. E-mail: tmaji@jncasr.ac.in; Tel: +91 80 2208 2826

† Electronic supplementary information (ESI) available: Experimental details. CCDC reference numbers 705856. For ESI and crystallographic data in CIF or other electronic format see DOI: 10.1039/b818498d

centres on the pore surface (Fig. 1b and S4).† There is also a small channel along the *b*-axis (3.1 × 2.2 Å^2) and no effective channel along the *a*–axis (Fig. S3).† The guest water molecules O3 and O4 are H-bonded (O3 ··· O4, 3.027 Å) to each other, and O3 also making a bridge between the two layers through N1 of the pendant CN group (N1 ··· O3, 2.944 Å). The guest 4,4′-bipy undergoes strong face to face and edge to face π–π interactions with two different coordinated 4,4′-bipy (cg ··· cg distances are in the range of 3.689–5.210 Å) linkers connected to Mn1 and Mn2 centres. In the 3D network, separation between the layers through Mn(II)-4,4′-bipy-Mn(II) is 11.628 Å while in the 2D layer, the Mn1–Fe1 and Mn2–Fe1 distances are 5.230 Å and 5.240 Å, respectively.

Thermogravimetric analysis of **1** was performed under a nitrogen atmosphere (Fig. S5)† and shows that the framework is stable up to 285 °C (see details in ESI).† Powder X-ray diffraction (PXRD) of the sample at 190 °C shows noticeable variations in the intensity of the reflections, accompanied by slight shifts of the Braggs peaks (Fig. S6).† This change corresponds to a small structural rearrangement upon the loss of the guest as well as the coordinated water molecules.

N_2 (77 K), CO_2 (195 K), and H_2 (77 K) sorption measurements were carried out in Quantachrome-1. Prior to the sorption measurement, the as-synthesized sample was treated at 473 K under vacuum and the resulting compound $\{[Mn_3(4,4'\text{-bipy})_3][Fe(CN)_6]_2\}_n$ (**1′**) was used for the sorption study. As shown in Fig. 2, the framework exhibits a typical type-II isotherm for N_2 (kinetic diameter, 3.6 Å)[10] and type-I profile for CO_2 (3.4 Å) and the surface areas calculated from Langmuir equation is about 20 m^2 g^{-1} and 157 m^2 g^{-1}, respectively. Hysteretic sorption with CO_2 molecules suggests strong interaction with the pore surfaces. The channels along the *b*-axis and square-shaped channel along the *c*-axis are smaller than the kinetic diameter of N_2 and CO_2 and the larger 1D channels are available for the adsorption which is realized by the smaller uptake of N_2 and CO_2. Hydrogen sorption at 77 K and up to 1 atm is found to be 0.52 wt% without saturation (Fig. S7).† The isosteric heat of hydrogen sorption is about 4.1 kJ mol^{-1}, which is comparable to other metal–organic systems.[5c,e] Table S1 shows H_2 uptake (wt%) *versus* specific surface area (<1000 m^2 g^{-1}) of porous coordination framework in the condition of 77 K and 1 atm and exhibits H_2 uptakes are substantially proportional to the specific surface area of porous coordination framework.† The greater deviation was observed for surface area >1000 m^2 g^{-1}.[5]

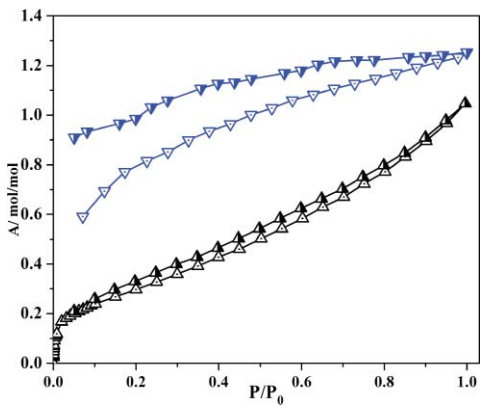

Fig. 2 N_2 (77 K, black) and CO_2 (195 K, blue) adsorption and desorption isotherms for **1′**. P_0 is saturated vapour pressure of the adsorbates.

Inspired by the two different channels with different size and chemical environment, we anticipated that **1′** could selectively adsorb solvents molecules on the basis of size and polarity. Water (H_2O), methanol (MeOH), acetonitrile (CH_3CN), ethanol (EtOH), and benzene (C_6H_6) vapor sorption isotherms were measured. As shown in Fig. 3, the sorption profiles of H_2O (kinetic diameter 2.8 Å), MeOH (4.0 Å) and CH_3CN (4.3 Å) reveal a type-I curve and steep uptake in the low P/P_0 region indicates strong affinity with the pore surfaces. The H_2O sorption profile (Fig. 3a) shows two step sorption, indicating different sorption sites in the framework. The large hysteresis in all cases is realized by the strong interaction and confinement on the pore surfaces decorated by the coordinative unsaturated Mn(II) sites and guest induced structural modification was displayed by the PXRD patterns (Fig. S6).† All the profiles were analyzed by the DR equation and suggesting 7.6, 3.08, and 1.89 molecules of H_2O, MeOH, and CH_3CN were adsorbed per formula unit of **1′**, respectively. The values of βE_0, which reflect adsorbate-adsorbent affinity, are 7.44 kJ mol^{-1}, 5.51 kJ mol^{-1}, and 3.79 kJ mol^{-1} for H_2O, MeOH, and CH_3CN, respectively, reflecting strong hydrophilic character of the pore surfaces. Very small uptake (saturated amount ~18 mL) and long diffusion time of the EtOH molecules can be correlated by the weak hydrophilicity and comparable size (kinetic diameter 4.8 Å) to the channel aperture of **1′** (Fig. 3d). Consistent with the smaller pore size, **1′** completely excludes benzene (C_6H_6) (kinetic diameter 5.8 Å) molecules at 298 K (Fig. 3e).

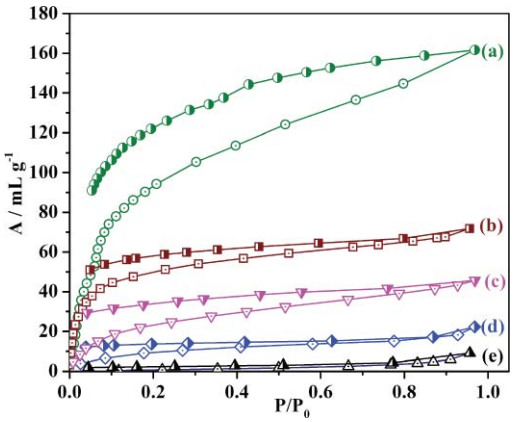

Fig. 3 Vapour sorption isotherm for **1′**. (a) H_2O (298 K); (b) MeOH (293 K); (c) CH_3CN (298 K); (d) EtOH (298 K) and (e) C_6H_6 (298 K). P_0 is the saturated vapour pressure of the adsorbates at respective temperature.

The magnetic properties of **1** are shown in Fig. 4 and exhibit that on lowering the temperature, $\chi_M T$ values ($\chi_M T$ at 300 K = 14.55 cm^3 mol^{-1} K) decreases and at around 45 K, $\chi_M T$ = 12.20 cm^3 mol^{-1} K and then it increases to 13.96 cm^3 mol^{-1} K at 20 K and finally it decreases to 7.93 cm^3 mol^{-1} K at 2.3 K. The Plot of $1/\chi_M$ *versus* T (Fig. 4) obeys the Curie–Weiss law in the temperature range 300–45 K with a Weiss constant θ = –13.24 K and a Curie constant C = 15.19 cm^3 mol^{-1} K (expected spin only value for three S = 5/2 Mn(II) and two low spin S = 1/2 Fe(III) centres is 13.87 cm^3 mol^{-1} K). The negative sign of the Weiss constant indicates antiferromagnetic exchange interactions as expected for Fe(III)–CN–Mn(II) bridges where there is direct

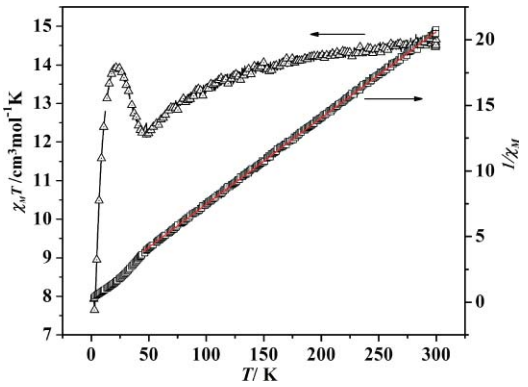

Fig. 4 Plot of $\chi_M T$ *versus* T and $1/\chi_M$ *versus* T for **1** in the temperature range of 300 to 2.5 K.

overlap of the t_{2g} magnetic orbitals.[3g,h] The sudden increase of $\chi_M T$ value at 45 K indicates the ferrimagnetic type behaviour due to the complete non-cancellation of spins, *i.e*, spin canting in the layers. Further connection of the layers through 4,4′-bipy induces antiferromagnetic interactions as indicated by decreases of the $\chi_M T$ value from 20 K. As Fig. S8 shows, the magnetization value gradually increases, but saturation is incomplete and far from the expected value at 5T (M = 7 $N\beta$ and the expected value is 13 $N\beta$) is consistent with the antiferromagnetic system.† Other reported 2D CN^- bridged Mn(II)–Fe(III) system shows ferrimagnetic ordering due to the competing interactions with some degree of spin canting.[3g,h] In this system the residual spin in the layers is further cancelled by 4,4′-bipy pillar module.

In summary, we have successfully designed and synthesized a novel 3D pillared-layer framework of Mn(II)–Fe(III) with two different channels by making use of a mixed inorganic $(Fe(CN)_6)^{3-}$ and organic (4,4′-bipy) ligand system. The framework shows permanent porosity and good H_2 storage capacity and the vapour sorption studies reveal strong hydrophilic pore surfaces and would be useful in discriminating the MeOH molecule from a mixture of MeOH and its higher homologues. Such bimetallic assembly using cynametallate inorganic and organic bridging linkers may open up a new route in fabricating porous magnetic materials. The detail study by changing $[M(CN)_6]^{n-}$ or organic linker is under progress, which will be reported as a full paper.

Acknowledgements

S. P is grateful to JNCASR for SRFP fellowship and T. K. M acknowledges the financial support from DST (fast track proposal). The authors are thankful to Dr G. Mostafa for valuable suggestions.

Notes and references

‡ *Crystal data* for **1**: FW = $C_{62}H_{54}Fe_2Mn_3N_{22}O_7$, M_w = 1495.74, Orthorhombic, space group *Pbam* (no. 55), a = 16.3148(8) Å, b = 17.8861(11) Å, c = 11.6284(6) Å, V = 3393.3(3) Å^3, Z = 2, ρ_{calc} = 1.458 g cm^{-3}, μ (Mo Kα) = 1.028 mm^{-1}, $F(000)$ = 1514, T = 100 K, λ (Mo Kα) = 0.7103 Å, θ_{max} = 24.9°, total data = 24 867, unique data = 3109, R_{int} = 0.109, observed data [$I > 2\sigma(I)$] = 2077, R = 0.0471, R_w = 0.1130, GOF = 1.02.

1 (*a*) O. M. Yaghi, M. O'Keeffe, N. W. Ockwig, H. K. Chae, M. Eddaoudi and J. Kim, *Nature*, 2003, **423**, 705; (*b*) S. Kitagawa, R. Kitaura and S.-I. Noro, *Angew. Chem., Int. Ed.*, 2004, **43**, 2334; (*c*) S. E. James, *Chem. Soc. Rev.*, 2003, **32**, 276; (*d*) C. Janiak, *Dalton Trans.*, 2003, 2781; (*e*) G. Férey, *Chem. Soc. Rev.*, 2008, **37**, 191; (*f*) D. Bradshaw, J. B. Claridge, E. J. Cussen, T. J. Prior and M. J. Rossenisky, *Acc. Chem. Res.*, 2005, **38**, 273; (*g*) D. J. Collins and H. -C. Zhou, *J. Mater. Chem.*, 2007, **17**, 3154.
2 (*a*) D. Maspoch, D. Ruiz-Molina and J. Veciana, *J. Mater. Chem.*, 2004, **14**, 2713; (*b*) N. Yanai, W. Kaneko, K. Yoneda, M. Ohba and S. Kitagawa, *J. Am. Chem. Soc.*, 2007, **129**, 3496; (*c*) W. Kaneko, M. Ohba and S. Kitagawa, *J. Am. Chem. Soc.*, 2007, **129**, 13706; (*d*) M. Kurmoo, H. Kumagai, K. W. Chapman and C. J. Kepert, *Chem. Commun.*, 2005, 3012.
3 (*a*) O. Kahn, Y. Pei, M. Verdaguer, J. P. Renard and J. Sletten, *J. Am. Chem. Soc.*, 1988, **110**, 782; (*b*) M. Verdaguer, *Science*, 1996, **272**, 698; (*c*) M. Ohba and H. Okawa, *Coord. Chem. Rev.*, 2000, **198**, 313; (*d*) W. Kaneko, S. Kitagawa and M. Ohba, *J. Am. Chem. Soc.*, 2007, **129**, 248; (*e*) O. Kahn, *Nature*, 1995, **378**, 667; (*f*) W. R. Entley and G. S. Griolani, *Inorg. Chem.*, 1994, **33**, 5165; (*g*) J. A. Smith, J.-R. Galán-Mascarós, R. Clérac and K. R. Dunbar, *Chem. Commun.*, 2000, 1077; (*h*) F. Bonadio, M.-C. Senna, J. Ensling, A. Seiber, A. Neels, H. Stoeckli-Evans and S. Decurtins, *Inorg. Chem.*, 2005, **44**, 969; (*i*) R. Podgajny, M. Bałanda, M. Sikora, M. Borowiec, L. Spałek, C. Kapusta and B. Sieklucka, *Dalton Trans.*, 2006, 2801.
4 (*a*) L. G. Beauvais and J. R. Long, *J. Am. Chem. Soc.*, 2002, **124**, 12096; (*b*) S. S. Kaye and J. R. Long, *J. Am. Chem. Soc.*, 2005, **127**, 6506.
5 (*a*) X. Lin, J. Jia, X. Zhao, K. M. Thomas, A. J. Blake, G. S. Walker, N. R. Champness, P. Hubberstey and M. Schröder, *Angew. Chem., Int. Ed.*, 2006, **45**, 7358; (*b*) A. G. Wong Foy, A. J. Matzger and O. M. Yaghi, *J. Am. Chem. Soc.*, 2006, **128**, 3494; (*c*) M. Latroche, S. Surblé, C. Serre, C. Mellot-Draznieks, P. L. Llewellyn, J. H. Lee, J. S. Chang, S. H. Jhung and G. Férey, *Angew. Chem., Int. Ed.*, 2006, **45**, 8227; (*d*) B. Panella, M. Hirscher, H. Pütter and U. Müller, *Adv. Funct. Mater.*, 2006, **16**, 520; (*e*) H. Chun, D. N. Dybtsev, H. Kim and K. Kim, *Chem.–Eur. J.*, 2005, **11**, 3521; (*f*) J. T. Culp, S. Natesakhawat, M. R. Smith, E. Bittner, C. Matranga and B. Bockrath, *J. Phys. Chem. C*, 2008, **112**, 7079.
6 (*a*) D. Bradshaw, T. J. Prior, E. J. Cussen, J. B. Claridge and M. J. Rosseinsky, *J. Am. Chem. Soc.*, 2004, **126**, 6106; (*b*) T. K. Maji, K. Uemura, H.-C. Chang, R. Matsuda and S. Kitagawa, *Angew. Chem., Int. Ed.*, 2004, **43**, 3269; (*c*) T. K. Maji, R. Matsuda and S. Kitagawa, *Nat. Mater.*, 2007, **6**, 142; (*d*) D. N. Dybtsev, H. Chun, S. H. Yoon, D. Kim and K. Kim, *J. Am. Chem. Soc.*, 2004, **126**, 32; (*e*) J.-P Zhang and X.-M. Chen, *J. Am. Chem. Soc.*, 2008, **130**, 6010; (*f*) J. T. Culp, M. R. Smith, E. Bittner and B. Bockrath, *J. Am. Chem. Soc.*, 2008, **130**, 12427.
7 (*a*) B. Chen, N. W. Ockwig, A. R. Milward, D. S. Contreras and O. M. Yaghi, *Angew. Chem., Int. Ed.*, 2005, **44**, 4745; (*b*) P. M. Forster, J. Eckert, J. S. Chang, S. E. Park, G. Férey and A. K. Cheetham, *J. Am. Chem. Soc.*, 2003, **125**, 1309; (*c*) M. Dincă, A. Dailly, Y. Liu, C. M. Brown, D. A. Neumann and J. Long, *J. Am. Chem. Soc.*, 2006, **126**, 16876.
8 (*a*) V. A. Blatov, A. P. Shevchenko and V. N. Serezhkin, *J. Appl. Crystallogr.*, 2000, **33**, 1193; (*b*) V. A. Blatov, L. Carlucci, G. Ciani and D. M. Proserpio, *CrystEngComm*, 2004, **6**, 377.
9 A. L. Speck, *PLATON*, The University of Utrecht, Utrecht, The Netherlands, 2001.
10 (*a*) D. W. Beck, *Zeolite Molecular Sieves*, Wiley & Sons, New York, 1974; (*b*) C. E. Webster, R. S. Drago and M. C. Zerner, *J. Am. Chem. Soc.*, 1998, **120**, 5509.

